

Optical Engineering

OpticalEngineering.SPIEDigitalLibrary.org

Analysis of laser damage tests on coatings designed for broad bandwidth high reflection of femtosecond pulses

John Bellum
Trevor Winstone
Laurent Lamaignere
Martin Sozet
Mark Kimmel
Patrick Rambo
Ella Field
Damon Kletecka

Analysis of laser damage tests on coatings designed for broad bandwidth high reflection of femtosecond pulses

John Bellum,^{a,*} Trevor Winstone,^b Laurent Lamaignere,^c Martin Sozet,^c Mark Kimmel,^a Patrick Rambo,^a Ella Field,^a and Damon Kletecka^a

^aSandia National Laboratories, P.O. Box 5800, MS 1197, Albuquerque, New Mexico 87185, United States

^bSTFC Rutherford Appleton Laboratory, Chilton, Didcot, Oxon, OX11 0QX, United Kingdom

^cCommissariat à l'Energie Atomique et aux Energies Alternatives, Centre d'Etudes Scientifiques et Techniques d'Aquitaine, 15 Avenue des Sablières—CS 60001, 33116 Le Barp Cedex, France

Abstract. We designed an optical coating based on TiO₂/SiO₂ layer pairs for broad bandwidth high reflection (BBHR) at 45-deg angle of incidence (AOI), P polarization of femtosecond (fs) laser pulses of 900-nm center wavelength, and produced the coatings in Sandia's large optics coater by reactive, ion-assisted e-beam evaporation. This paper reports on laser-induced damage threshold (LIDT) tests of these coatings. The broad HR bands of BBHR coatings pose challenges to LIDT tests. An ideal test would be in a vacuum environment appropriate to a high energy, fs-pulse, petawatt-class laser, with pulses identical to its fs pulses. Short of this would be tests over portions of the HR band using nanosecond or sub-picosecond pulses produced by tunable lasers. Such tests could, e.g., sample 10-nm-wide wavelength intervals with center wavelengths tunable over the broad HR band. Alternatively, the coating's HR band could be adjusted by means of wavelength shifts due to changing the AOI of the LIDT tests or due to the coating absorbing moisture under ambient conditions. We had LIDT tests performed on the BBHR coatings at selected AOIs to gain insight into their laser damage properties and analyze how the results of the different LIDT tests compare. © The Authors. Published by SPIE under a Creative Commons Attribution 3.0 Unported License. Distribution or reproduction of this work in whole or in part requires full attribution of the original publication, including its DOI. [DOI: 10.1117/1.OE.56.1.011012]

Keywords: optical coatings; broad bandwidth high reflection; high laser-induced damage thresholds.

Paper 160635SSP received Apr. 27, 2016; accepted for publication Aug. 1, 2016; published online Aug. 25, 2016.

1 Introduction

This paper is based on a conference proceedings paper.¹ Its context is that of large-scale petawatt (PW) high energy lasers whose pulses are of durations in the femtosecond (fs) regime.² These pulses are comprised of broad spectral ranges of frequency components whose relative phases determine the pulse shape.³ Our particular interest is in optical coatings, which we have designed and produced⁴ to be suitable for broad bandwidth high reflection (BBHR) at 45-deg angle of incidence (AOI), and P polarization (Ppol) of PW-class fs laser pulses with 900-nm center wavelength, such as the fs pulses of the Vulcan Laser at the Central Laser Facility in the United Kingdom.⁵

A standard requirement for such BBHR coatings is that they should provide reflectivity exceeding 99.5% as well as low group delay dispersion (GDD) over the entire spectrum of the fs pulses they are to reflect, so that the pulses do not suffer distortion or broadening of their temporal profiles on reflection.³ Furthermore, because the BBHR coatings are important for reflection of high intensity fs pulses of PW lasers by their final off-axis parabola and fold mirrors, their laser-induced damage thresholds (LIDTs) must be high enough to ensure the mirrors will perform in the environment and under the laser pulse conditions of the actual PW laser beam train. In this regard, our BBHR coating design goal was ambitious, guided by achieving $R > 99.5\%$, GDD within ± 20 fs², and LIDT > 800 mJ/cm² for 45-deg

AOI, Ppol over a 200-nm operational band with 900-nm center wavelength, i.e., from 800 to 1000 nm.⁴

The resulting design, which was based on TiO₂/SiO₂ layer pairs, did not completely meet these R and GDD goals, but did afford $R > 99.5\%$ from 801 to 999 nm and GDD within ± 20 fs² from 823 to 949 nm and rising smoothly to ~ 3500 fs² at 800 nm and dropping smoothly to ~ -3500 fs² at 1000 nm.⁴ We considered this to be acceptable because the HR band of 198 nm is close to the 200 nm goal, and the smooth GDD variation with wavelength is favorable to techniques for compensating large GDD (such as > 20 fs²) where it occurs over the operational band.

BBHR coatings based on this design were produced in Sandia's large optics coating chamber^{6,7} by means of e-beam evaporation with ion-assisted deposition (IAD). Results of the measurements of these R and GDD behaviors for the initial coating that we produced were encouraging, exhibiting $R > 99.5\%$ over a 213-nm band with 967-nm center wavelength, and smoothly varying GDD within ± 100 fs² over that wavelength band.⁴ By recalibrating that initial coating run, we produced the BBHR coatings of this paper, which we report in Sec. 3 and have HR band center wavelengths close to 900 nm according to the choice of ambient environment. The details of the design and production of these coatings, including the choice of TiO₂ and SiO₂ for the layers, are provided in Sec. 3 and by the earlier report,⁴ which also discusses the GDD and temporal distortion effects on fs pulses in detail.

This brings us to the third aspect of our BBHR coatings; namely, their LIDTs, the challenges in measuring and verifying them, and whether they meet the above goal of

*Address all correspondence to: John Bellum, E-mail: jbellu@sandia.gov

$>800 \text{ mJ/cm}^2$ for fs pulses. LIDT tests of the BBHR coatings play a critical role in determining whether they are suitable for use. In this paper, we will explore some of the issues associated with LIDT tests of BBHR mirror coatings designed for fs pulses, focusing in particular on differences in the environments, pulse durations and wavelengths between available LIDT test lasers and large-scale PW-class lasers in which the BBHR coatings must perform.

2 Dilemmas in LIDT Tests of BBHR Coatings

A major dilemma in LIDT testing of BBHR coatings is that available LIDT test lasers and test environments often do not match the actual PW-class lasers and their use environments. We discuss first the issue of environment, including ambient versus vacuum conditions for LIDT testing, and the effect on LIDTs of water absorption in coatings.

PW-class laser beam trains prior to final focusing of the high intensity fs pulses are in a vacuum environment.² This is because, in any other ambient pressure environment, the high power fs pulse fluences at or near foci, such as those of spatial filters, would lead to deleterious nonlinear effects, such as self-focusing or intensity clamping, which would compromise the interaction of the pulses with a target at final focus. On the other hand, available LIDT tests are often performed in ambient environments rather than in vacuum. This is mostly a matter of the convenience of not dealing with the complications of vacuum environments. It is also valid in that the fluences of LIDT test lasers, whether or not the tests require a focused beam, only need to exceed the damage thresholds of the coatings, and those thresholds, except for extremely high LIDT optical materials, are below the thresholds for nonlinear processes in ambient incident media.

While nonvacuum test environments are valid because most coating LIDTs are below thresholds for deleterious nonlinear phenomena in ambient gaseous media, they nevertheless can affect LIDT outcomes. One way this may happen has to do with possible shifts of transmission/reflection spectra of BBHR coatings in humid ambient environments in comparison to dry air or vacuum environments. Another way has to do with the possible interaction of the ambient gases themselves with a coating through absorption and/or desorption processes that cause it to exhibit an LIDT that differs between ambient and vacuum environments. This paper addresses the former ambient-versus-vacuum LIDT differences. The latter ambient-versus-vacuum LIDT phenomena are, however, important and warrant a discussion, which follows.

Several specific studies⁸⁻¹¹ have explained vacuum-ambient LIDT differences primarily in terms of the amount of water absorbed from an ambient environment by a coating, especially one that is less dense/more porous. Two studies were for pulses in the fs regime and specific to single layers of HfO_2 and SiO_2 deposited by ion-beam sputtering (IBS), with 50 fs LIDT test laser pulses of 800-nm center wavelength and 1-kHz pulse repetition rate (PRR).^{8,9} These LIDT tests with 50 fs pulses showed that 1-on-1 LIDTs remained the same between vacuum and ambient conditions. The multiple-pulse LIDTs in vacuum proved, however, to be much less than the 1-on-1 LIDTs in comparison to their counterparts at atmospheric pressure. The studies went on to attribute this to the absence in vacuum of not only water vapor in the vicinity the films but also water absorbed

by the films, with either or both of these absences of water causing higher oxygen deficiency in the films that in turn enhances incubation effects,^{12,13} such as accumulation of laser-induced electronic defects, associated with multiple-fs-pulse damage processes.

Another study focused on pulses in the ns regime and specific to six-layer $\text{Ta}_2\text{O}_5/\text{SiO}_2$ and $\text{Nb}_2\text{O}_5/\text{SiO}_2$ antireflection coatings deposited by IBS and IAD and non-IAD e-beam evaporation, with ns LIDT test laser pulses at 355 nm and 100 Hz PRR, and at 1064 nm and 10 Hz PRR.¹⁰ For these ns pulses, the 1-on-1 and multiple-pulse LIDTs were similar in air and vacuum environments for the higher density (IBS and IAD) and also lower density (non-IAD) coatings in the case of the tests at 1064 nm, but only for the higher density (IBS and IAD) coatings in the case of the tests at 355 nm. The study attributed the ambient-vacuum LIDT similarity for the higher density coatings to their low absorption of water, making their amorphous structures free of water whether they are in air or vacuum.¹⁰ For the less dense, non-IAD coatings, the LIDTs in vacuum were less than those in air for the tests at 355 nm while the air-vacuum LIDTs were similar for the tests at 1064 nm. This difference between the ns pulses at 355 and 1064 nm was, according to the study, due to higher water absorption by the non-IAD coatings, with water absorbed by them under ambient conditions altering their conductivity and/or stress properties in ways favorable to higher LIDTs in comparison to in vacuum for 355 nm but not 1064 nm.¹⁰ This may also have to do with the different photon energies and laser damage mechanisms for these wavelengths. The ns pulses at both wavelengths cause damage predominantly controlled by extrinsic defects at the nanoscale level, but intrinsic damage due to excitation of native electronic state defects can also occur, with lesser (greater) likelihood for the lower photon energy, 1064 nm (higher photon energy, 355 nm) pulses. It may be that the conductivity and stress effects of water absorbed by the porous, non-IAD coatings also stabilize them with respect to excitation of their native electronic state defects, thus favoring intrinsic damage, especially by the higher energy photon 355 nm pulses, in air compared to in vacuum.

Our in-house study¹¹ focused on pulses in the sub-picosecond (ps) regime and specific to 34-layer and 50-layer $\text{HfO}_2/\text{SiO}_2$ coatings designed for HR at 30-deg and 35-deg AOIs, respectively, and deposited by e-beam evaporation with IAD, with 1-on-1 LIDT tests of the coatings at the design AOIs in Ppol using laser pulses of 400 fs duration, 1053-nm center wavelength, and 10 Hz PRR. This study found no change in the LIDTs between tests in air and in vacuum, which is consistent with the other studies⁸⁻¹⁰ for 1-on-1 tests on higher density, IAD or IBS, coatings.

Overall, these studies indicate that, for higher density IAD or IBS multilayer dielectric coatings, measurements of 1-on-1 LIDTs for pulses ranging from the fs to the ns regimes will likely provide the same or similar results for vacuum and ambient conditions, regardless of the relative humidity (RH) of the ambient conditions. This probably would not be the case for multiple-pulse LIDTs or for lower density/more porous, non-IAD coatings, especially if the ambient conditions are humid, since these vacuum-ambient LIDT differences correlate strongly with the absence (in vacuum) or presence (under ambient conditions) of water vapor and absorption of water by the coatings.⁸⁻¹⁰ It is not clear from

these studies whether the latter vacuum-ambient LIDT differences depend only on water vapor being part of the ambient environment. This could mean that they may not be as strong or even evident at all when the ambient environment is dry (0% RH). Certainly, there is a need for further research into vacuum-ambient LIDT differences. In any case, most available LIDT tests take place in air at the ambient humidity of the test laboratory, though more LIDT testing facilities are beginning to offer tests in dry (0% RH) air or nitrogen ambient environments as well as in vacuum. The 34-layer and 50-layer HR coatings for non-normal AOI of our in-house study¹¹ are more similar to the multilayer BBHR coatings for 45-deg AOI, Ppol of this paper than are the single layer and six-layer coatings of the other studies.⁸⁻¹⁰ This holds promise that the lack of vacuum-ambient LIDT differences of our in-house study will also apply to the BBHR coatings of this paper. Nevertheless, it is important to be aware that results of any LIDT tests in ambient environments may differ from those of tests in vacuum.

We now turn to the environmental issue concerning the wavelength shifts of transmission/reflection spectra of BBHR coatings in humid ambient environments in comparison to the spectra in dry air or vacuum environments. This phenomenon is due to absorption by the coating of water from humid environments. As we have mentioned, IAD and IBS can lead to coatings that can be dense enough that they absorb little if any water. As a result, they may exhibit essentially no spectral shifts in humid environments.

On the other hand, the HfO_2 and SiO_2 IBS single layers of one of the above studies^{8,9} did exhibit evidence of water absorption and, as we will show, the IAD $\text{TiO}_2/\text{SiO}_2$ BBHR coatings of this paper also exhibit spectral shifts due to absorption of water. We have observed a trend with our coatings that such spectral shifts increase in amount as the number of coating layers or their thickness increases, which is consistent since more or thicker layers can absorb more water. The $\text{TiO}_2/\text{SiO}_2$ BBHR coatings of this study, because of their many layers, exhibit significant spectral shifts in humid environments, and we present examples of these spectral shifts later in the paper. As a result of such spectral shifts, the coating's HR band under ambient conditions may no longer match its design HR band. More importantly, it may no longer match the spectrum of the PW-class laser's fs pulses. So, while it is usually a goal for an LIDT test laser to have a pulse spectrum matching that of the PW-class laser, realizing that goal is of little or no value if the LIDT tests are done in an ambient environment in which the HR band of the BBHR coating has shifted beyond the fs pulse spectrum.

This issue of mismatch between center wavelengths and spectra of the pulses of available LIDT test lasers and of the fs PW-class lasers as well as the HR band of the BBHR coatings is critical to LIDT testing of BBHR coatings. Figure 1 shows this for scenarios of a PW-class laser with 25 fs pulses at a center frequency, ν_o , and corresponding center wavelength, λ_o , and 25 fs, 300 fs and 1 nanosecond (ns) LIDT test laser pulses, some of whose center frequencies

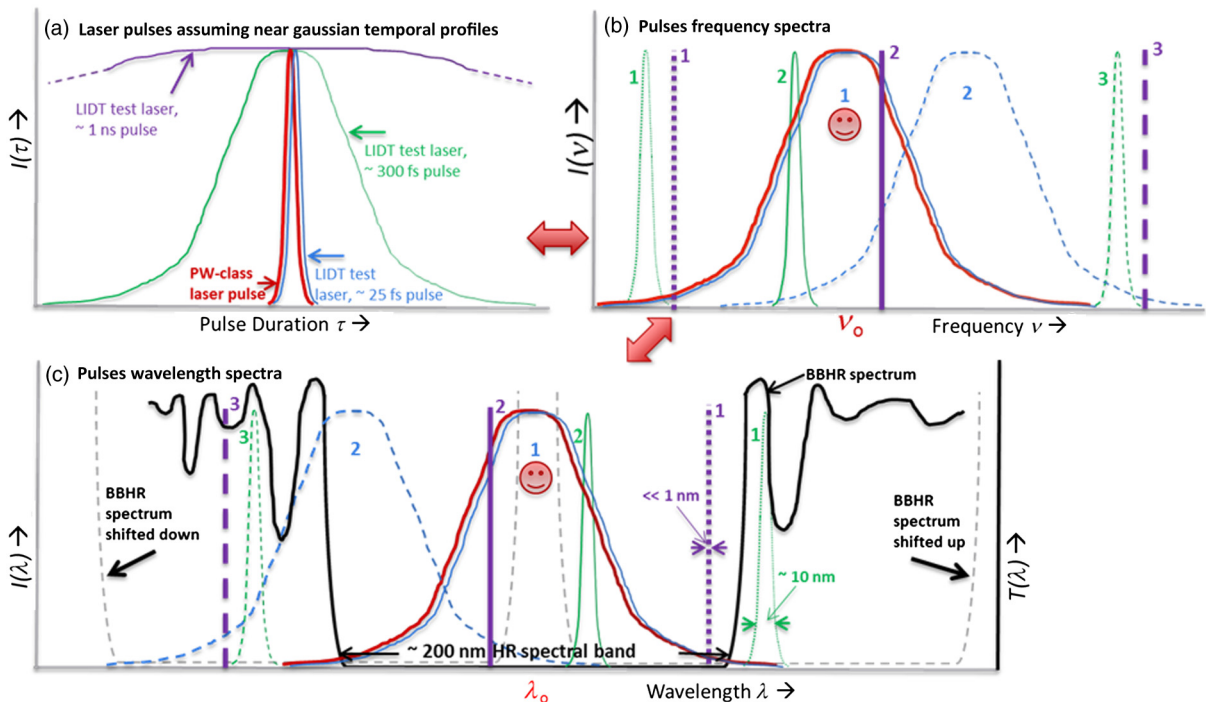


Fig. 1 Illustrations of (a) temporal profiles of a 25-fs PW-class laser pulse (red line) and 25 fs (blue line), 300 fs (green line) and 1 ns (purple line) LIDT test laser pulses; (b) frequency spectra of the pulses for different LIDT test laser center frequencies (indicated by line style and labels 1, 2, or 3, with ν_o marking the PW-class laser center frequency); and (c) wavelength spectra of the pulses (with λ_o marking the PW-class laser center wavelength), and BBHR coating transmission spectra with 200 nm HR band centered at λ_o (black line) and shifted in wavelength (gray dashed lines) down (BBHR spectrum shifted down) or up (BBHR spectrum shifted up). Smiley faces highlight the case of a match of the PW and LIDT test laser pulses in both duration and λ_o/ν_o .

(wavelengths) match ν_o (λ_o) while others do not. For our illustration, we assume near Gaussian temporal profiles for the pulses, as shown in Fig. 1(a). Possible corresponding frequency and wavelength spectra of these pulses are depicted in Figs. 1(b) and 1(c), respectively. The assumption of near Gaussian temporal profiles of the pulses is reasonable, but means that we are not illustrating situations in which the laser pulses exhibit skewed temporal or spectral profiles due to gain compensation or frequency chirping pulse shaping techniques.³

Consider the scenario of LIDT test lasers with 25 fs pulses. This would be the ideal LIDT test situation in that it allows testing the laser damage properties of the BBHR coating with fs pulses whose duration matches that of the PW laser pulses. Laser damage with such fs pulses would be primarily intrinsic, associated with multiphoton ionization mechanisms due to direct interaction of the high intensity fs pulse photons with the coating layer materials.¹³ We show two cases in Figs. 1(b) and 1(c): case 1, highlighted by a smiley face, in which the LIDT test laser pulse spectrum exactly overlaps that of the fs PW-class laser and also the HR band of a BBHR coating having a 200-nm HR band with center wavelength, λ_o , as shown in Fig. 1(c); and case 2 in which the LIDT test laser pulse spectrum is shifted to a higher center frequency (lower center wavelength) than that of the fs PW-class laser or the HR band of the BBHR coating. For case 1 to occur would be very fortunate, since it is rare that an available LIDT test laser has pulses as well as center wavelength that exactly match those of the fs PW laser. Case 1 would mean that the entire spectrum of the fs pulse overlaps within the coating's HR band. For standard quarter-wave HR coatings, the E-field behavior for incident light of wavelengths within the central zone of the HR band is characterized by intensity peaks that quench rapidly into the coating layers.¹⁴ Near quarter-wave HR coatings also exhibit this E-field behavior. Quenching of E-field intensity peaks into the coating persists out to wavelengths near its HR band edge but in a more gradual way, with appreciable intensities occurring deeper within the stack of coating layers. Our earlier paper⁴ shows examples of this E-field behavior for the BBHR coating design of this study, and other examples appear later in this paper. Such quenching of E-field intensity into the coating is favorable to higher LIDTs because only a small number of outer coating layers encounter high E-field intensities. However, as we have pointed out above, even case 1 does not ensure valid LIDT tests of the BBHR coating if they are performed in a humid environment in which the HR band shifts with respect to the fs pulse spectrum. This latter situation is similar to case 2 described earlier. In both situations, the test laser pulse has part of its spectrum at wavelengths for which the BBHR coating exhibits high transmission. LIDTs in tests of a BBHR coating with such offsets between the laser pulse spectrum and the coating's HR band will be lower than when the center wavelengths of the pulse and the HR band of the coating match. This is because, when the center wavelengths are offset, only a part of the pulse spectrum probes the coating's HR band while the other part probes the coating at wavelengths of high transmission outside its HR band, and thus, penetrates at moderate to high electric field intensities all the way through the coating layers resulting in increased likelihood of laser damage. Therefore, it is important in laser damage

tests for the pulse and coating HR band center wavelengths to be the same or nearly the same in order to avoid obtaining misleadingly low LIDTs.

The option of performing LIDT tests with fs PW-class lasers themselves is very unlikely because these are large-scale laser systems dedicated to non-LIDT-test purposes.² Taking them off line and configuring them for LIDT tests would be prohibitively expensive in terms of both time and cost. For fs lasers in general, there are three basic center wavelength options:² 1054 nm (or 1030 nm) based on Nd:glass gain media; 910 nm based on optical parametric chirped pulse amplification using KDP, DKDP, or LBO crystals pumped by the frequency-doubled output of Nd:glass gain media;⁵ and 800 nm based on Ti:Sapphire laser technology. Of these, Ti:Sapphire-based lasers are the most available. This leaves limited prospects for obtaining LIDT tests with fs pulses of center wavelengths other than 800 nm and gives motivation to consider what might be learned about the laser damage characteristics of a BBHR coating from LIDT tests with more readily available lasers having longer, ns, ps, or sub-ps pulses. Figure 1 shows two examples of such LIDT test options, with LIDT test laser pulses of 300 fs and 1 ns and center wavelengths within and outside the spectrum of the 25 fs PW laser pulses. Laser damage with these longer-duration pulses is due to a range of mechanisms ranging from intrinsic damage, especially in the sub-ps pulse regimes, to damage in the ns regime controlled by extrinsic defects from contamination or structural anomalies at the nanoscale level in the coating layers.¹³ This mix of damage mechanisms offers some promise that it may be possible to at least gain insight into, if not quantitative estimates of, fs laser damage behaviors from LIDT tests with longer pulses.

While the spectrum of a fs PW laser pulse spans most if not all of the HR band of an appropriately designed BBHR coating, the bandwidths of 300 fs and 1 ns pulses are in the range of 10 nm and <1 nm, respectively, as shown in Fig. 1(c). Thus, LIDT tests with 300 fs or 1 ns pulses could probe the laser damage behavior of a BBHR coating in 10 nm or <1 nm, respectively, segments of its HR band. To conduct such tests over the entire HR band would, of course, require some way of tuning the center wavelengths of these long-pulse LIDT test lasers across the HR band of the BBHR coating. Another option would be to shift the HR band of the BBHR coating with respect to the LIDT test laser's center wavelength. This could be accomplished by changing the AOI for the LIDT tests compared to the design AOI of the BBHR coating. This could also be accomplished by controlling the humidity of an ambient LIDT test environment. Such shifts of the HR band are shown in Fig. 1(c), which shows the cases of the BBHR spectrum shifted down or up in wavelength to allow the spectra of LIDT test lasers with center wavelengths offset from λ_o to overlap the HR band. Such shifted HR bands would expand options for LIDT tests of the BBHR coating within its HR band using available LIDT test lasers of pulse lengths matching or longer than that of the fs PW laser, and whose pulse spectra would otherwise completely or partially overlap with wavelengths of high transmission of the unshifted BBHR transmission spectrum. Regarding this latter approach to shifting the HR band, we refer back to the discussion earlier in this section regarding evidence that coatings with absorbed water in humid

environments may exhibit higher LIDT compared to in vacuum environments.⁸⁻¹⁰

The preceding possibilities raise questions about the validity and usefulness of LIDT tests of a BBHR coating with shifted HR bands and with laser pulses different from the fs PW laser pulses in center wavelength and/or in pulse duration. We address several of these questions. First, do LIDT tests with longer, sub-ps, ps, or ns pulses have value regarding fs pulse laser damage behavior? Yes, they do, because studies have shown that there are trends in LIDTs going from longer, ns pulses down to the fs pulse regime.^{13,15-17} It is true, as we have already pointed out, that the laser damage mechanisms for these pulse regimes differ, from intrinsic, nonlinear processes, such as multiphoton ionization, directly related to the characteristic of the dielectric material (bandgap) for the fs to ps regimes,^{13,17} to laser absorption by extrinsic, embedded defects for the ns regime.¹⁸ Nevertheless, the LIDT trends between these regimes indicate that there may be varying degrees of influence from intrinsic and extrinsic mechanisms depending on pulse duration, meaning that LIDT behavior in one pulse regime may be at least partially characteristic of LIDT behavior in another pulse regime.

Next, do LIDT tests at different AOIs from that of the BBHR coating design have value? Yes, they do, because E-fields for quarter-wave type HR coatings at wavelengths within their HR bands at AOIs different from the design AOI behave similarly to E-fields within the HR band at the design AOI. This E-field behavior, which we have mentioned above, is characterized by intensity peaks that quench into the coating layers,¹⁴ and is favorable to higher LIDTs. This is not to say that the relationship between LIDT and AOI is straightforward. E-field intensity peaks, especially in the outer few layers of HR coatings, can vary in strength depending on AOI, leading to LIDTs at one AOI that may be higher or lower than at another AOI. The LIDT behaviors at different AOIs should vary in similar ways depending, e.g., on variation of the center wavelength of the LIDT test laser pulses. Another factor regarding LIDT tests at different AOIs is that, as AOI increases, projected fluence on coating layers decreases as cosine of the AOI, favoring higher LIDT while optical path in the coating layers increases also as cosine of the AOI, favoring lower LIDT. Though these geometrical effects depend on other factors such as how many layers play a strong role in the reflection process, they nevertheless do influence LIDTs in opposite ways as AOI changes, and may reduce differences between LIDTs measured at one AOI compared to those measured at another AOI.

A further question is the following. Do LIDTs for HR bands shifted in wavelength from the spectrum of the PW-class laser pulses have value? Yes, they do, based on the E-field behaviors over HR bands as mentioned above. There is, however, a caution to take into account in comparing LIDTs for shifted HR bands; namely, band-gap related intrinsic laser damage may be higher (lower) for HR bands that are shifted to lower (higher) wavelengths from the spectrum of the PW laser pulses. Finally, if the use environment is vacuum, do LIDT tests in humid ambient environments have value? Yes, they do, because, according to the studies of vacuum-ambient LIDT differences⁸⁻¹¹ that we reviewed above, the LIDTs of coatings in vacuum and ambient environments will likely be the same or similar at least for 1-on-1 LIDT

tests in the case of higher density, IAD or IBS, multilayer dielectric coatings.

3 Coatings for BBHR at 45 Deg, Ppol of fs Pulses with 800 to 1000 nm Spectra

We explore LIDT test issues of the previous section using BBHR coatings that we described in Sec. 1 for 45-deg AOI and Ppol. The fs pulses of interest to us have a center wavelength of 900 nm with spectra extending from 800 to 1000 nm; as we have explained in Sec. 1, our coating design was guided by achieving $R > 99.5\%$ and low GDD for 45-deg AOI, Ppol over the spectral range of 800 to 1000 nm, in keeping with standard BBHR requirements. The coatings consisted of TiO₂/SiO₂ layer pairs produced by e-beam evaporation with IAD in Sandia's large optics coating chamber.^{6,7} For the TiO₂ layers, we used an O₂ back pressure in the chamber and reactively evaporated Ti metal. The details of the deposition process, the choice of SiO₂ and TiO₂ as the low and high index layer materials, respectively, and the BBHR design process appear in our earlier report.⁴ Here, we mention that we chose SiO₂ for the low index layer material because of its refractive index, at ~ 1.46 , that is one of the lowest among transparent oxides, and its high, ~ 8.3 eV, band-gap that makes it resistant to laser damage. We needed a high index layer material of very high refractive index to achieve an index contrast ratio with SiO₂ high enough to meet the demanding reflectivity requirement of $R > 99.5\%$ from 800 to 1000 nm. The drawback is that high index dielectric materials have low band-gaps, which are not favorable to high LIDTs. We chose TiO₂ for the high index layers despite its low, ~ 3.3 eV, band-gap because its high refractive index, at ~ 2.47 , affords an index contrast ratio with SiO₂ that is high enough to meet the design requirements for the HR band. Our BBHR coating design softens the deleterious LIDT effects of the low band-gap TiO₂ layers in that the peak intensities of the standing wave E-fields across the broad HR band are lower at the TiO₂ layers than they are at the high band-gap SiO₂ layers. The design was optimized by starting from quarter-wave layer thicknesses in a reverse chirped arrangement to meet the HR requirements while maintaining low GDD. It features a thick (\sim half-wave) outer layer of SiO₂. Again, more details of the design and deposition processes appear in our other report,⁴ which also presents the results of a white light interferometric measurement of the initial BBHR coating's GDD. As we mentioned in Sec. 1, this GDD data exhibit low values with smooth behavior over the coating's HR band, appropriate for preserving the temporal profile of fs pulses on reflection.

Figure 2 shows the design and measured transmission spectra of the BBHR coating as deposited in Run 072, the coating run that produced the coating for use in a dry (0% RH) ambient environment or in vacuum. All of the measured spectra in this study were made using a PerkinElmer Lambda 950 spectrophotometer. In the case of Fig. 2, the spectral measurement was under 0% RH conditions provided by a dry air purge in the sample compartment of the Lambda 950. This 0% RH environment is the one for which the coating's transmission spectrum most closely matches what it would be in vacuum due to the fact that the coating in both dry and vacuum environments is free of absorbed water. The transmission spectrum of Fig. 2 shows that the coating meets

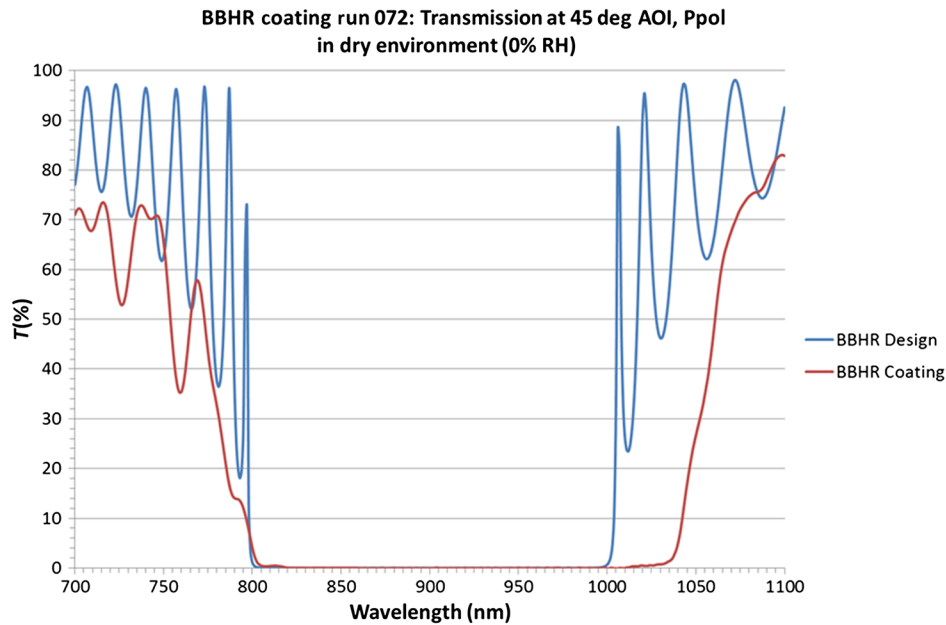


Fig. 2 Transmission spectrum as measured under dry (0% RH) conditions at 45-deg AOI, Ppol for the BBHR coating of Run 072, shown in comparison to the coating's corresponding design transmission spectrum.

the design reflectivity performance requirement quite well, providing $R > 99.5\%$ at 45-deg AOI, Ppol, over a 213-nm band from 805 to 1018 nm.

Figure 3 shows the measured transmission spectra of this Run 072 coating for 0-deg AOI, and in Ppol for 45-deg and 65-deg AOIs, at 0% RH and 50% RH conditions in the Lambda 950 sample compartment. The HR band for $R > 99.5\%$ is shown below the spectral graphs of Fig. 3 for each measured spectrum. Figure 4 shows a similar set of measured transmission spectra for a BBHR coating of the same design but deposited in Run 071, a different coating run in which we set the layer thickness calibration factors with a goal of

producing a coating that meets the design HR band requirement of $R > 99.5\%$ from 800 to 1000 nm at 45-deg AOI, Ppol under 50% RH conditions. Run 071 was largely successful in achieving this goal as Fig. 4 confirms, with $R > 99.5\%$ extending from 799 to 987 nm for the coating's 45° AOI, Ppol transmission spectrum under 50% RH conditions. A trend evident in Figs. 3 and 4 is that the HR band of a BBHR coating decreases as AOI increases.

Figure 5 shows the transmission spectrum of the Run 071 coating at 0% RH, 15% RH, and 50% RH for 45-deg AOI, Ppol as an example of how the spectrum shifts with respect to RH for a given AOI. The spectra of Figs. 3–5 show the range

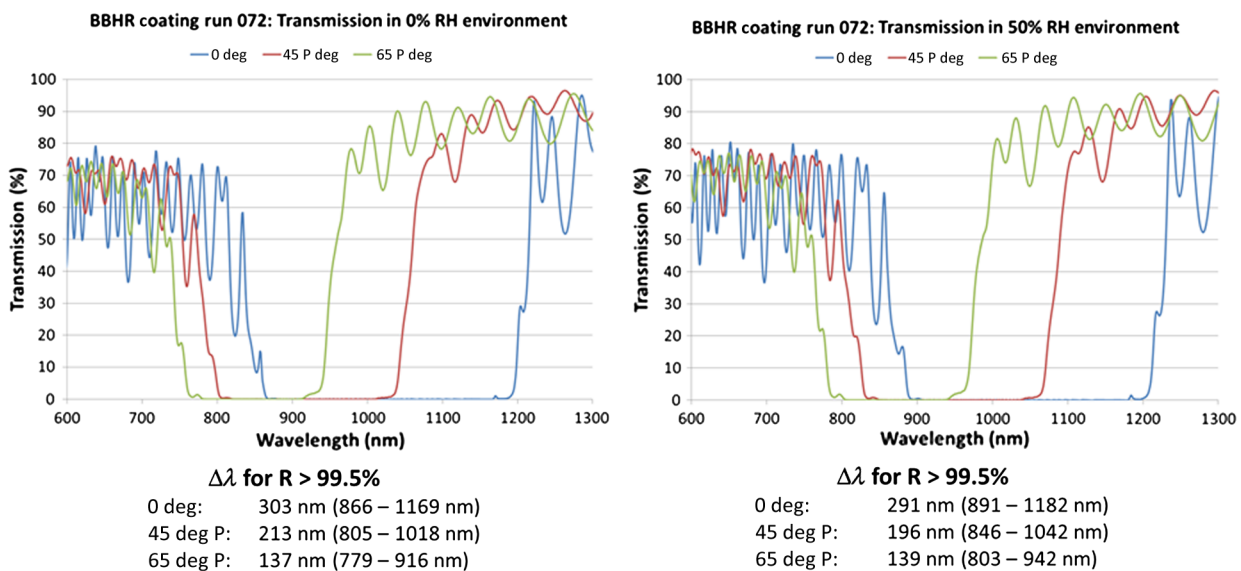


Fig. 3 Measured transmission spectra of the BBHR coating of Run 072 for 0-deg AOI, and for 45-deg and 65-deg AOIs, Ppol, at 0% RH and 50% RH ambient conditions. The HR band, $\Delta\lambda$, for $R > 99.5\%$ is shown below the graphs for each measured spectrum.

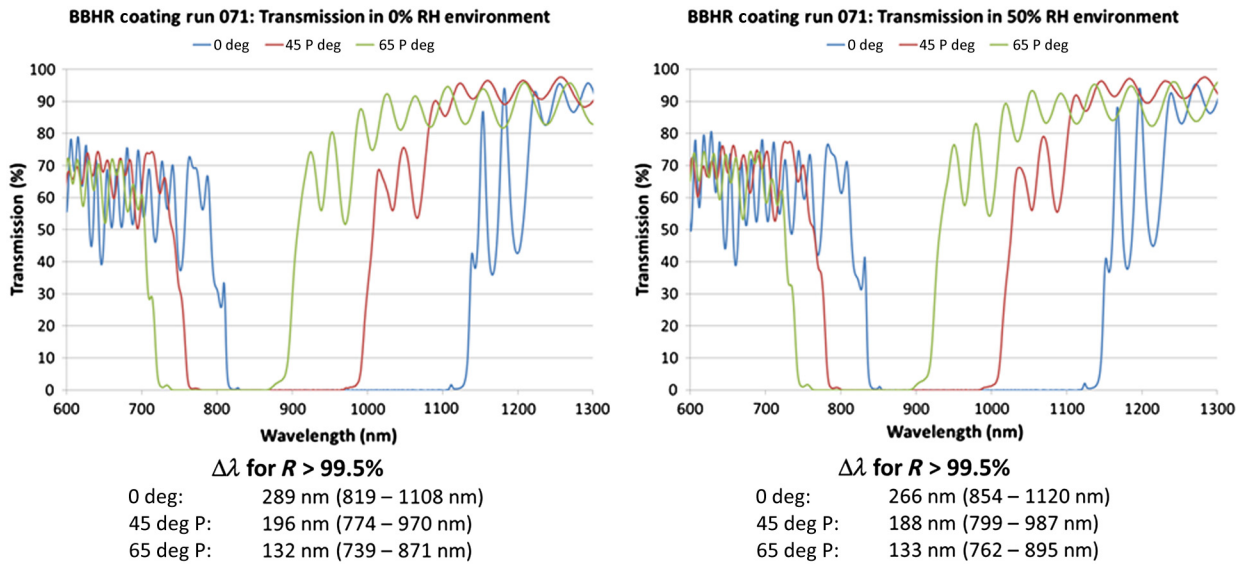


Fig. 4 Measured transmission spectra of the BBHR coating of Run 071 for 0 deg AOI, and for 45-deg and 65-deg AOIs, Ppol, at 0% RH and 50% RH ambient conditions. The HR band, $\Delta\lambda$, for $R > 99.5\%$ is shown below the graphs for each measured spectrum.

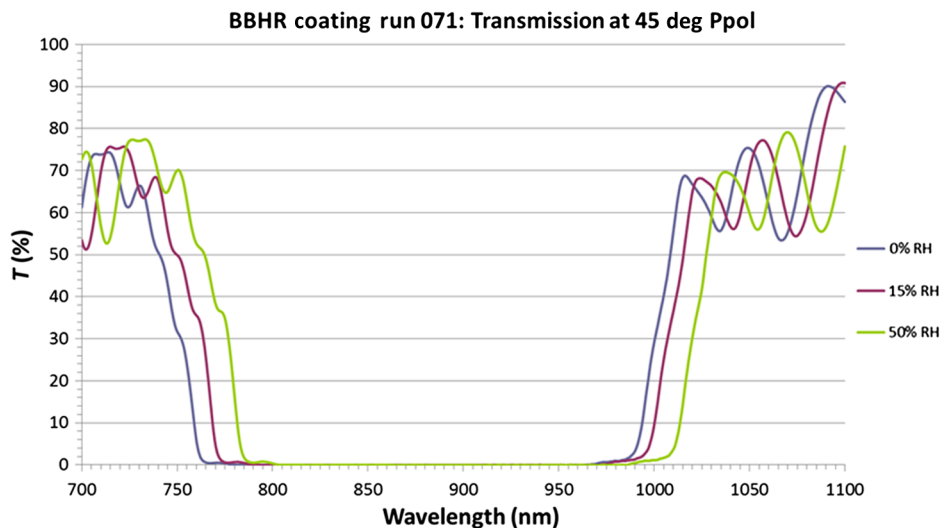


Fig. 5 Measured transmission spectra of the BBHR coating of Run 071 at 45-deg AOI, Ppol, under 0%, 15%, and 50% RH conditions.

of HR bands available for LIDT tests of the coating under different conditions of ambient humidity and at different AOIs. In practice, shifting the HR band of a coating by setting and maintaining specific ambient humidity levels requires sophisticated monitoring and closed loop feedback control of RH, which is expensive and not easy to achieve. We managed, with considerable difficulty, to obtain the transmission scans with the Lambda 950 spectrophotometer under the 15% and 50% RH conditions by introducing into the sample compartment a combination of dry air and air made humid due to moisture arising from a container of warm water. On the other hand, setting AOI of LIDT tests at specific values is easy to achieve. For this reason, we decided to use AOI as a means of shifting the HR band of our BBHR coatings for LIDT tests under dry (0% RH) or nearly dry conditions.

4 LIDT Tests of the BBHR Coating of Run 072

LIDT tests of the BBHR coating of Run 072 were performed by CEA-CESTA in France using the laser test facility called DERIC¹⁹ with 675 fs pulses of 1053-nm center wavelength and a 1/e focal spot diameter on the coating surface of 155 μm . These were 1-on-1 and 10-on-1 tests based on the ISO 21254-2 protocols,²⁰ and the laser PRR was 10 Hz. Fluence values have an absolute accuracy better than 10% as determined by the error margin of the measuring instruments. The LIDT is given by the mean between the highest fluence for which no damage occurs and the lowest fluence for which the damage probability is nonzero. The uncertainty is specified by a calculation of the difference between this average value and these two fluences. The test environment was within an enclosure under ambient conditions that were

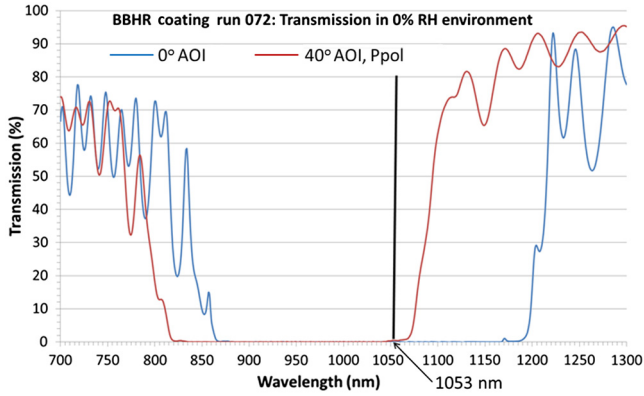


Fig. 6 Measured transmission spectra of the BBHR coating of Run 072 at 0-deg AOI and at 40-deg AOI, Ppol, under dry (0% RH) conditions. The thick black vertical line indicates 1053 nm, the center wavelength of the CEA-CESTA 675 fs LIDT test laser pulses. It is well within the central zone of the HR band for 0-deg AOI and near the HR band edge for 40-deg AOI, Ppol.

nearly dry, at ~20% RH. The LIDT tests were at normal incidence (0-deg AOI) in order to probe the coating in the central part of its HR band and at 40-deg AOI, Ppol, in order to probe the coating near the long wavelength edge of its HR band. Figure 6 shows the location of the LIDT test laser center wavelength, 1053 nm, within the HR bands for 0-deg and 40-deg AOIs, Ppol. Figure 7 shows the BBHR coating design E-field intensities for 1053 nm at 0-deg AOI and at 40-deg AOI, Ppol for the spectral conditions corresponding to those of Fig. 6 for the Run 072 coating. These E-field intensity plots are similar to those at 45-deg AOI of the earlier report,⁴ which explains in detail the Spol and Ppol effective refractive indices for the high and low index layers of quarter-wave HR coatings. These effective indices are responsible not only for HR band center wavelengths shifting lower with increasing AOI but also for the broadening of

Spol HR bands and narrowing of Ppol HR bands as AOI increases. At the center wavelengths of HR bands, the effective layer indices have quarter-wave structure for HR with shallow E-field penetration into the coatings. This E-field penetration increases at wavelengths near the HR band edge because effective indices match those for quarter-wave HR structure less and less for wavelengths nearer and nearer the HR band edge. The result, in this case, is that the intensities of the 1053 nm E-fields of Fig. 7 for 40-deg AOI penetrate deeper into the coating layers for Ppol than for Spol because 1053 nm is at the edge of the 40-deg AOI, Ppol HR band (see Fig. 6), but not of the 40-deg AOI, Spol HR band (not shown in Fig. 6) because it is broader than its Ppol counterpart. These and the 0-deg AOI E-fields of Fig. 7 are examples of how the E-field intensity peaks quench less rapidly into coating layers at wavelengths near the edge of the HR band than they do within its central spectral zone. We are interested in comparisons between LIDT behaviors at wavelengths not only well within the HR band's central zone and near its edge but also between its central zone and edge. LIDT differences between these situations may be associated with corresponding differences of the E-field behaviors in the coating, as we have discussed in Sec. 2.

Figure 8 shows plots of damage probability versus laser fluence for the CEA-CESTA 1-on-1 and 10-on-1 LIDT tests at 0-deg AOI and at 40-deg AOI, Ppol. We measure fluences in the laser beam cross section, normal to the beam propagation direction, regardless of AOI of the LIDT test, and report the fluence of a laser shot in terms of normal beam fluence. According to the ISO standard,²⁰ it corresponds to the energy density at the top of the Gaussian transverse beam intensity profile, and we calculate it as the ratio of the total energy in the beam to the effective beam area (set as the area at 1/e for a Gaussian beam).²¹ In all cases in Fig. 8, the transition of the damage probability from 1 to 0 is very sharp, indicating that the damage is primarily intrinsic, governed by the coating materials' electronic properties rather than

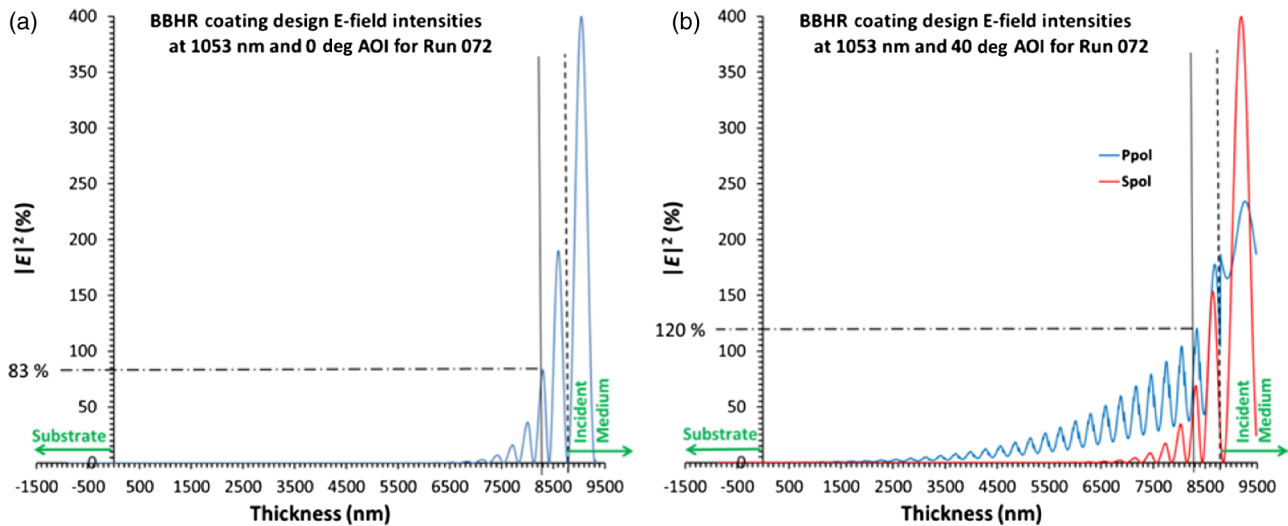


Fig. 7 BBHR coating design E-field intensities at 1053 nm in the coating layers as a percentage of incident intensity under spectral and humidity conditions corresponding to those of Fig. 6 for the Run 072 coating. (a) The E-fields at 0-deg AOI are for the central zone of the HR band and (b) at 40-deg AOI are for the edge of the HR band. In each graph, the dashed line marks the boundary of the coating with the incident medium; the solid line marks the interface between the outermost TiO₂ layer (to the right of the line) and the next-to-outermost SiO₂ layer (to the left of the line); and the dash-dot line marks the peak E-field intensity in the outermost TiO₂ layer.

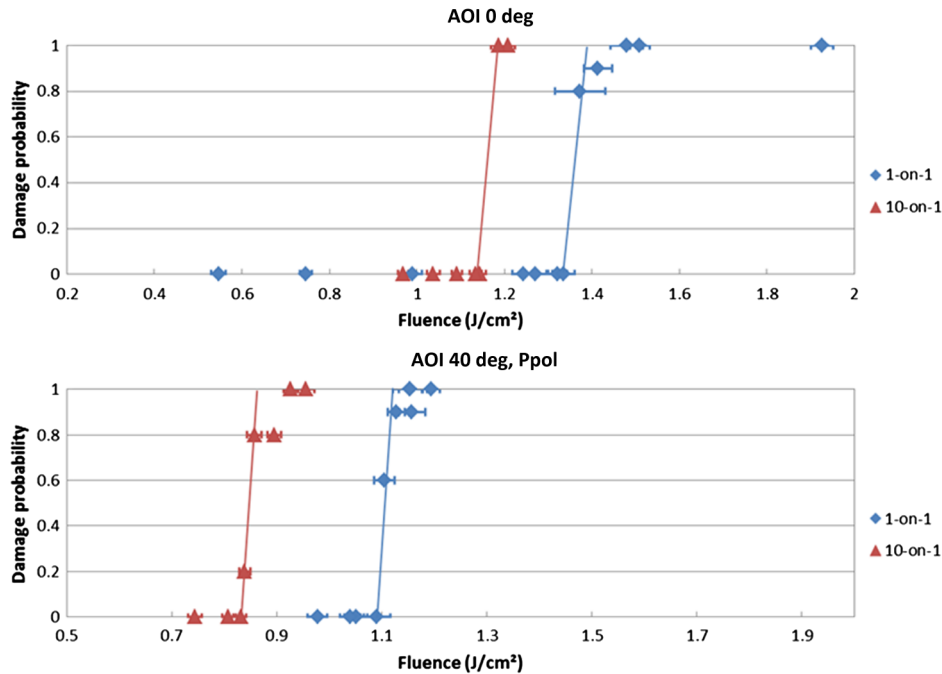


Fig. 8 Damage probability versus fluence for 1-on-1 and 10-on-1 LIDT tests of the BBHR coating of Run 072, as measured by CEA-CESTA at 0-deg AOI and at 40-deg AOI, Ppol with 675 fs laser pulses of 1053-nm center wavelength. Solid lines are guides for the eyes. At 0-deg AOI, the 1-on-1 and 10-on-1 LIDTs are 1.35 ± 0.02 and 1.17 ± 0.02 J/cm², respectively. At 40-deg AOI, Ppol, the 1-on-1 and 10-on-1 LIDTs are 1.10 ± 0.01 and 0.83 ± 0.01 J/cm², respectively.

by structural or nanoscale defects in the coating. This, in fact, is what we expect for laser damage caused by 675 fs pulses.

The respective 1-on-1 and 10-on-1 LIDTs are higher for 0-deg AOI than for 40-deg AOI, Ppol. This is counterintuitive considering that the projected fluence on the coating is lower and would favor higher LIDT at 40-deg AOI than at 0-deg AOI. We conclude that these results are related to the differences in E-field behaviors shown by Fig. 7 between the central and edge spectral zones of the HR band. In all cases of Fig. 7, the highest E-field intensity peaks within the coating are in its thick, approximately half-wave, outer SiO₂ layer, so are unlikely to drive laser damage because of the high band-gap of SiO₂. The next-highest E-field intensity peaks occur in the outermost TiO₂ layer and are more important to laser damage because of the low band-gap of TiO₂. As Fig. 7 shows, these latter peaks are ~120% and ~83% of the incident intensity for 40-deg AOI, Ppol (i.e., for the HR band edge) and 0-deg AOI (i.e., for the central part of the HR band), respectively. Therefore, we might expect the 1-on-1 LIDTs for these two cases to be in the ratio of 120/83 (=1.45) but, in fact, their ratio, 1.35/1.1 (see Fig. 8), is less, at 1.23. This could be because the E-field intensity peak is very close to the interface between the outermost TiO₂ and next-to-outermost SiO₂ layers for 0-deg AOI, while it is further from this layer interface and well within the outermost TiO₂ layer for 40-deg AOI, Ppol (see Fig. 7). Because the layer interface tends to have more native nanoscale structural and electronic state defects, the peak's proximity to it for 0-deg AOI could lead to that LIDT being lower than the peak intensity alone would indicate, thus accounting for the LIDT ratio being 1.23 rather than 1.45.

The decrease of LIDT between the 1-on-1 and 10-on-1 tests (see Fig. 8) is ~14% (from 1.35 ± 0.02 J/cm² to

1.17 ± 0.02 J/cm²) for 0-deg AOI (i.e., for the central part of the HR band) while it is larger, ~25% (from 1.10 ± 0.01 to 0.83 ± 0.01 J/cm²), for 40-deg AOI, Ppol (i.e., for the edge of the HR band). We attribute the difference between the 1-on-1 and 10-on-1 LIDTs to incubation effects^{12,13} that we mention above, in Sec. 2, such as formation of electronic state defects in material when irradiated by multiple pulses. This incubation effect is independent of laser PRR up to around 1 kHz (our tests are at a PRR of 10 Hz), and the resulting electronic state defects are not reversible; i.e., they persist once they form. The incubation effect appears to be stronger at 40-deg AOI, Ppol than at 0-deg AOI. This is consistent with the deeper penetration into the coating of strong E-field intensity peaks for 40-deg AOI, Ppol (see Fig. 7), which would lead to a higher probability of creation of electronic state defects in the coating. Though our interest is in Ppol, we note that the Spol E-field intensities for 40-deg AOI are similar to the E-field intensities and for 0-deg AOI (see Fig. 7), except that the intensity peak in the outermost TiO₂ layer is less (70% of incident intensity) and well within the layer for 40-deg AOI, Spol while it is greater (83% of incident intensity) and near the layer's interface with the next-to-outermost SiO₂ layer for 0-deg AOI. Therefore, we would expect the 1-on-1 and 10-on-1 LIDTs for 40-deg AOI, Spol to be similar to or somewhat higher than those for 0-deg AOI.

As an additional aspect of the LIDT results for 675 fs laser pulses, we present in Fig. 9 morphology images of damage sites for the 1-on-1 and 10-on-1 tests at 0-deg AOI and at 40-deg AOI, Ppol. These morphology measurements were made by CEA-CESTA in its Optical Metrology Laboratory. In each test case, the figure shows damage at a fluence slightly above the LIDT, where the damage has just begun to occur,

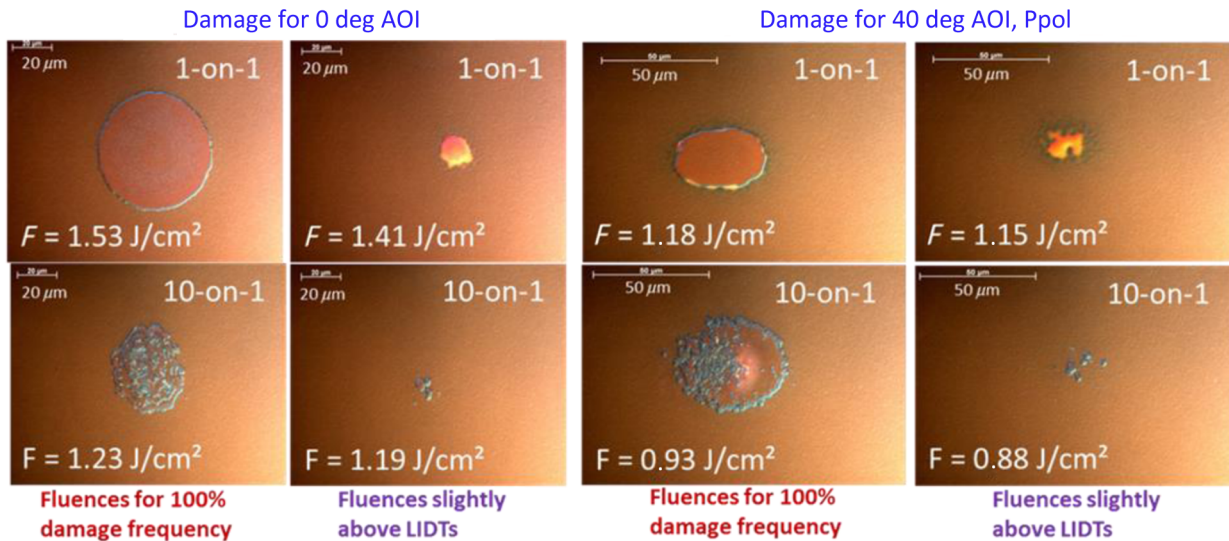


Fig. 9 Morphology images of laser-induced damage caused by 675-fs pulses at 1053 nm on the BBHR coating of Run 072 at 0-deg AOI and at 40-deg AOI, Ppol in 1-on-1 and 10-on-1 tests and with fluences as indicated.

and at a higher fluence, just high enough for the damage to occur with 100% frequency. The morphologies show a sharp increase of damage diameter over these fluence increases of just a few tenths of a J/cm², consistent with the sharp transition of the damage probability from 0 to 1 shown by the damage frequency results of Fig. 8. The 10-on-1 morphologies of Fig. 9 show evidence of the incubation effects that we mentioned above in that initial damage occurs not only at lower fluences, consistent with the lower 10-on-1 LIDTs, but also smaller in size when it occurs. All damage morphologies of Fig. 9 indicate delamination of the outer coating layers. The morphologies for 1-on-1 tests at fluences for 100% damage frequency are consistent with an analysis showing that, for these 675 fs pulses, the damage site dimensions correlate well with the irradiating pulses' transverse dimensions beyond which their Gaussian-distribution fluences are below the corresponding 1-on-1 LIDTs. The details of this analysis appear in a report²² that includes its application to the Run 072 coating (under the name, broad bandwidth mirror, in the report), and that explains how it forms the basis of a monoshot method of determining LIDTs using morphology images. Overall, we find these LIDT results for 675 fs laser pulses at 1053 nm to be encouraging.

5 LIDT Tests of the BBHR Coating of Run 071

LIDT tests of the BBHR coating of Run 071 were performed by Spica Technologies, Inc.²³ applying the NIF-MEL protocol²⁴ in the case of 800 and 8 ps pulses at a center wavelength of 1064 nm. These were single longitudinal and transverse mode pulses with Gaussian temporal and transverse intensity profiles. The test environment was within an enclosure maintained at 0% RH by means of a nitrogen purge. The tests were at 0-deg and 19-deg AOIs, Ppol. Figure 10 shows where the test laser center wavelength, 1064 nm, is located within the HR bands of the Run 071 coating at 0-deg and 19-deg AOIs, Ppol. The E-field plots of Fig. 11 are like those of Fig. 7 but, in this case, the wavelength is near the edge and in between the central zone and edge of the HR band. The intensity peaks quench rapidly into the coating layers in both

cases with the former showing a slightly higher intensity peak in the outermost TiO₂ layer than the latter (114% compared to 100% of incident intensity) and penetrating only slightly more into the coating. The 19-deg AOI, Ppol NIF-MEL LIDT tests probed close to the coating's HR band edge (see Fig. 10) but not as close as for the 40-deg AOI, Ppol LIDT tests of the Run 072 coating (see Fig. 6). As a result, the E-field intensity peaks in the latter case are higher and penetrate significantly further into the coating than in the former case (compare Figs. 7 and 11). The 0-deg AOI NIF-MEL LIDT tests probed the coating in between the HR band's central and edge zones (see Fig. 10) while the 0-deg AOI LIDT tests of the Run 072 coating probed the coating well within the central zone of its HR band (see Fig. 6). The differences here are less. The intensity peaks quench rapidly into the coating layers in both cases with the former showing only slightly higher peak intensity in the outermost TiO₂ layer than the latter (100% compared to 83% of incident intensity)

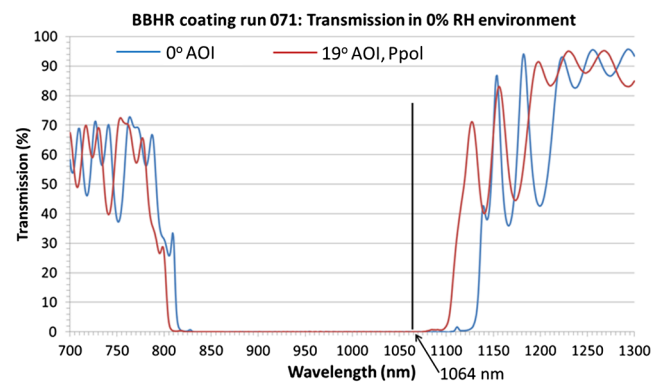


Fig. 10 Measured transmission spectra of the BBHR coating of Run 071 at 0-deg AOI and at 19-deg AOI, Ppol under dry (0% RH) conditions. The thick black vertical line indicates 1064 nm, the center wavelength of the NIF-MEL 800 and 8 ps LIDT test laser pulses. It is between the central zone and edge of the HR band for 0-deg AOI, and near the HR band edge for 40-deg AOI, Ppol.

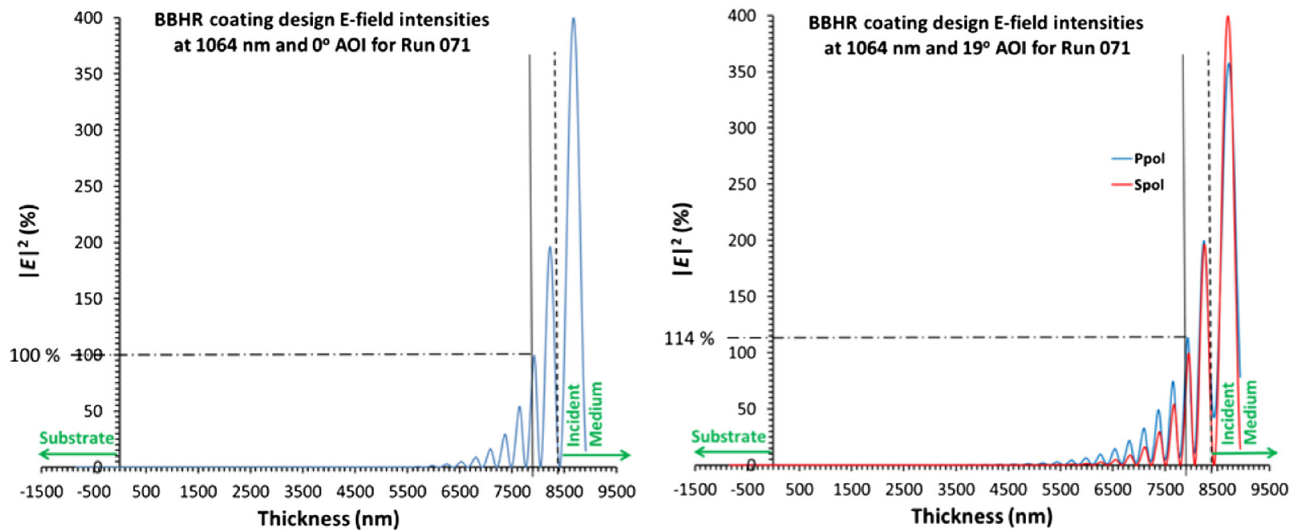


Fig. 11 BBHR coating design E-field intensities at 1064 nm in the coating layers as a percentage of incident intensity under spectral and humidity conditions corresponding to those of Fig. 10 for the Run 071 coating. The E-fields at 0-deg AOI are for in between the central zone and edge of the HR band (left-hand graph) and, at 19-deg AOI, are for near the edge of the HR band (right-hand graph). In each graph, the dashed line marks the boundary of the coating with the incident medium; the solid line marks the interface between the outermost TiO_2 layer (to the right of the line) and the next-to-outermost SiO_2 layer (to the left of the line); and the dash-dot line marks the peak E-field intensity in the outermost TiO_2 layer.

and penetrating only slightly more into the coating (compare Figs. 7 and 11).

In the NIF-MEL procedure, there is a sequence of raster scans of the focused laser beam over an area of 1 cm^2 of the coating. Each raster scan is focal spot by focal spot at a single fluence level with a single laser shot per focal spot site. The first scan starts at a low fluence, and each scan thereafter is at an increasingly higher fluence level. A camera detects damage, site by site, that is nonpropagating (i.e., that occurs but does not grow) as well as propagating (i.e., that occurs and grows), and LIDT is determined by the fluence level at which either the accumulated number of nonpropagating damage sites exceeds 1% of the total number of raster scan sites, or propagating damage occurs at one or more sites, whichever is the lower fluence.

For these LIDT tests, the 8 and 800 ps pulses had $1/e^2$ transverse intensity profile diameters at focus of 23 and $82 \mu\text{m}$, respectively, and, after each vertical scan, the substrate adjusted horizontally for the next vertical scan such that the separation of adjacent vertical scan lines equaled the diameter of the pulses' transverse Gaussian intensity profile at 90% of the peak intensity. In the case of the 800 ps pulses, the PRR was 20 Hz, and the vertical scan rate maintained a site-to-site separation that is the same as the separation between adjacent vertical scan lines. This arrangement made for a dense array of scan sites over the 1 cm^2 area, with the same high density of sites along vertical and horizontal lines of the array, and with significant overlap of the transverse intensity distributions of pulses at adjacent sites. In the case of the 8 ps pulses, the PRR, at 10 kHz, was 500 times higher than for the 800 ps pulses. The vertical scan rate was also much higher, but not high enough to maintain a site-to-site separation along the vertical scan direction that matches the separation between adjacent vertical scan lines. As a result, the density of scans sites along a vertical line of the array was very high for the 8 ps pulses, and higher than

its counterpart along a horizontal line of the array, which means that these pulses had much stronger overlap of their transverse intensity distributions between adjacent vertical scan sites than the 800 ps pulses.

Both propagating and nonpropagating damage by ns pulses is usually related to extrinsic coating defects that serve as initiation sites for damage mechanisms that occur on ns time scales. For ps and sub-ps pulses, coating defects play a role in nonpropagating damage behavior to a lesser extent or not at all,^{21,25} and propagating damage primarily results from intrinsic damage mechanisms based on direct interaction of the laser radiation with the coating layer materials. Figure 12 shows the 800- and 8-ps pulse NIF-MEL LIDT results in the form of a plot of cumulative number of nonpropagating damage sites versus fluence, with arrows indicating the fluences at which propagating damage occurs. As can be seen, all LIDTs of Fig. 12 are due to propagating damage. For the tests with 800 ps pulses, the LIDT at 0-deg AOI (at a spectral zone between the HR band's central and edge zones) is 11 J/cm^2 , and is higher than the 9 J/cm^2 LIDT at 19-deg AOI, Ppol (at wavelengths near the HR band edge). Also, the cumulative number of nonpropagating damage sites is 15 for the tests at 19-deg AOI compared to six for the tests at 0-deg AOI. This is consistent with the behaviors of the E-fields discussed earlier and shown in Fig. 11, which have higher peak intensities deeper into the coating layers and consequently sample more layer defects at wavelengths closer to the edge of the HR band. It is not surprising that we see some nonpropagating damage with the 800 ps pulses because this pulse duration is in the ns range of time scales for defect-related mechanisms of nonpropagating damage.

For the tests with 8 ps pulses, Fig. 12 shows no nonpropagating damage sites. This means that, for each raster scan at fluences less than the respective threshold fluences, no damage occurred; for the raster scans at the threshold

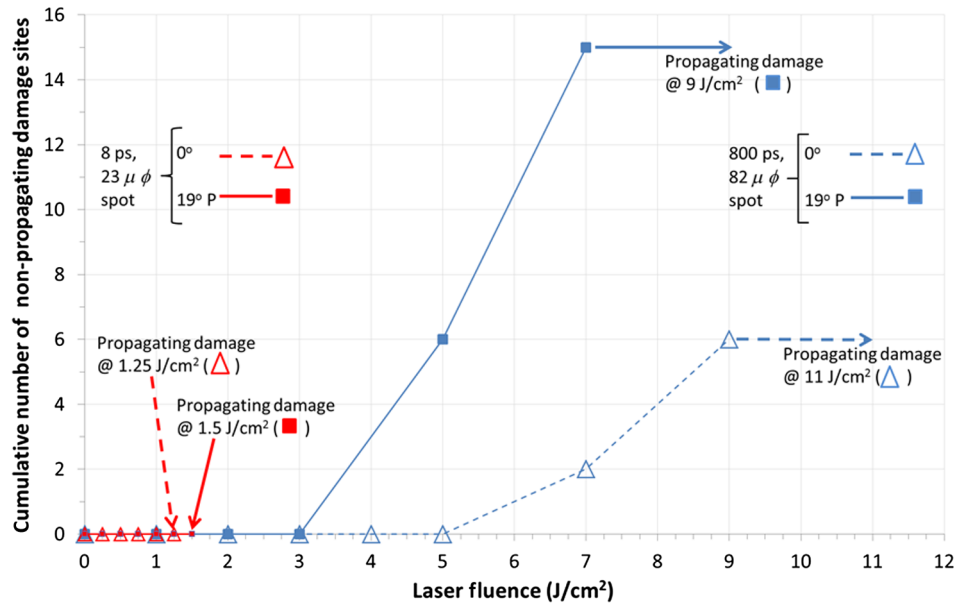


Fig. 12 Cumulative number of nonpropagating laser-induced damage sites versus laser fluence for NIF-MEL LIDT tests of the BBHR coating of Run 071 with 800 and 8 ps laser pulses of 1064-nm center wavelength at 0-deg AOI and at 19-deg AOI, Ppol. Arrows point to fluences at which propagating damage occurred. The triangle and square symbols indicate data points, and each data point for a particular fluence is from a raster scan of the laser pulses at that fluence over a 1-cm² area of the coating.

fluences of 1.25 J/cm² for 0-deg AOI and 1.5 J/cm² for 19-deg AOI, Ppol, damage occurred at least at one raster-scan site and continued to grow when the focal spot of the laser advanced to the next or a neighboring site. Because of the high density of scan sites for the 8 ps pulses and the high degree of their site-to-site overlap (as we have explained above), it is highly likely that this type of propagating damage actually occurred multiple times, rather than just once, during the scans at the threshold fluences. Regardless, this propagating damage is characteristic of intrinsic rather than defect-related mechanisms. We might expect this for the shorter, 8 ps pulses as compared to the longer, 800 ps (~1 ns) pulses, although defects in coating layer structures may strongly enhance E-field intensities and promote damage even in the short pulse regime.²⁶ To reiterate, propagating damage refers to damage that grows at one or multiple damage sites, and the propagating damage in the case of the 8 ps pulses most likely occurred at multiple sites because of the strong overlap of those pulses site-to-site in the vertical scan direction. Even so, by the NIF-MEL protocol, propagating damage at only one site is sufficient to set the LIDT.

Unlike the case of 800 ps pulses, the 8 ps pulse LIDT of 1.25 J/cm² for 0-deg AOI (at a spectral zone between the HR band's central and edge zones) is similar to, but a bit lower than the 1.5 J/cm² LIDT for 19-deg AOI, Ppol (near the HR band edge). This is, however, consistent with the intrinsic nature of the 8 ps pulse laser damage and with the fairly similar E-field behaviors for 0-deg and 19-deg AOIs, Ppol. Also, the NIF-MEL LIDTs for 8 ps pulses at 1064 nm (see Fig. 12) are about the same as or a bit higher than the ISO 21254-2 LIDTs for 675 fs pulses at 1053 nm (see Fig. 8), and are consistent, both in magnitude and in pulse-duration trend, with LIDTs of TiO₂ films for pulses of 800-nm center wavelength.¹⁵ This close similarity of LIDT values and pulse-duration trends indicates that the results of

Figs. 8 and 12 provide a reasonable characterization of the laser damage behavior of the BBHR coatings.

6 Summary and a Proposal

We have highlighted dilemmas in LIDT testing of BBHR coatings arising from differences between LIDT test lasers and test environments compared to fs PW-class lasers and their vacuum environment. We then argue the value of LIDT tests of BBHR coatings using available fs-to-ns laser pulses with AOI and RH shifts of coatings' HR bands to make them match the spectra of the LIDT test laser pulses. LIDT tests of coatings produced by Sandia's large optics coater according to the coating design for BBHR at 45-deg AOI, Ppol with 200 nm HR band centered at 900 nm and low GDD⁴ serve as examples of our suggested approach of using available LIDT test lasers to gain insight into laser damage characteristics of BBHR coatings. These tests were under dry or nearly dry conditions with HR bands shifted by means of AOI tuning, and used a 675-fs, 1053-nm laser, and 8 and 800 ps, 1064-nm lasers. Tuning of the AOI for the BBHR coating allowed our LIDT tests to probe laser damage behaviors at wavelengths within the central zone of the HR band, near the HR band edge, and between these two spectral zones of the HR band. We emphasize that these LIDT tests have value in providing comparisons of laser damage behaviors for different spectral zones of the HR band and in confirming pulse scaling trends from the ns to 675 fs pulse regimes, but allow only speculative, relative estimation of LIDTs for pulse durations in the few tens of fs regime. Further LIDT tests would be necessary before we would even speculate on values for fs LIDTs of our BBHR coatings. To this end, we propose the use of a laser with 350 fs pulses, whose center wavelength is tunable by means of optical parametric amplification, in order to conduct 45-deg AOI, Ppol

LIDT tests in vacuum of our BBHR coating in ~10 nm band intervals from 800 to 1000 nm.

Acknowledgments

This paper is based in part on an invited talk presented by one of us (J. C. B.) at the Pacific Rim Laser Damage 2015; Optical Materials for High Power Lasers Conference in Shanghai, China. Sandia National Laboratories is a multiprogram laboratory managed and operated by Sandia Corporation, a wholly owned subsidiary of Lockheed Martin Corporation, for the US Department of Energy's National Nuclear Security Administration under contract DE-AC04-94AL85000.

References

1. J. Bellum et al., "Analysis of laser damage tests on a coating for broad bandwidth high reflection of femtosecond pulses," *Proc. SPIE* **9532**, 953211 (2015).
2. C. Danson et al., "Petawatt class lasers worldwide," in *High Power Laser Science and Engineering*, Vol. 3, e3, pp. 1–14 (2015).
3. M. Wollenhaupt et al., "Femtosecond laser pulses: linear properties, manipulation, generation and measurement," Chapter 12 in *Springer Handbook of Lasers and Optics*, F. Traeger, Ed., pp. 937–983, Springer, New York (2007).
4. J. C. Bellum et al., "Low group delay dispersion optical coating for broad bandwidth high reflection at 45° incidence, P polarization of femtosecond pulses with 900 nm center wavelength," *Coatings* **6**, 11 (2016).
5. C. Hernandez-Gomez et al., "The Vulcan 10 PW project," *J. Phys. Conf. Ser.* **244**, 032006 (2010).
6. J. Bellum et al., "Meeting thin film design and production challenges for laser damage resistant optical coatings at the Sandia large optics coating operation," *Proc. SPIE* **7504**, 75041C (2009).
7. J. Bellum et al., "Production of optical coatings resistant to damage by petawatt class laser pulses," in *Lasers—Applications in Science and Industry*, K. Jakubczak, Ed., InTech, pp. 23–52 (2011).
8. D. N. Nguyen et al., "Studies of femtosecond laser induced damage of HfO₂ thin films in atmospheric and vacuum environments," *Proc. SPIE* **7504**, 750403 (2009).
9. D. N. Nguyen et al., "Femtosecond pulse damage thresholds of dielectric coatings in vacuum," *Opt. Express* **19**, 5690–5697 (2011).
10. L. Jensen et al., "Damage threshold investigations of high power laser optics under atmospheric and vacuum conditions," *Proc. SPIE* **6403**, 64030U (2006).
11. M. Kimmel et al., "Optical damage testing at the Z-Backlighter facility of Sandia National Laboratories," *Proc. SPIE* **7504**, 75041G (2009).
12. M. Mero et al., "On the damage behavior of dielectric films when illuminated with multiple femtosecond laser pulses," *Opt. Eng.* **44**(5), 051107 (2005).
13. W. Rudolph et al., "Laser damage in thin films—what we know and what we don't," *Proc. SPIE* **8885**, 888516 (2013).
14. P. W. Baumeister, *Optical Coating Technology*, pp. 5-51–5-55, SPIE Press, Bellingham, Washington (2004).
15. B. C. Stuart et al., "Nanosecond-to-femtosecond laser-induced breakdown in dielectrics," *Phys. Rev. B* **53**, 1749–1761 (1996).
16. A. Tien et al., "Short-pulse laser damage in transparent materials as a function of pulse duration," *Phys. Rev. Lett.* **82**, 3883–3886 (1999).
17. M. Mero et al., "Scaling laws of femtosecond laser pulse induced breakdown in oxide films," *Phys. Rev. B* **71**, 115109 (2005).
18. C. J. Stolz, M. D. Feit, and T. V. Pistor, "Laser intensification by spherical inclusions embedded within multilayer coatings," *Appl. Opt.* **45**, 1594–1601 (2006).
19. M. Sozet et al., "Laser damage density measurement of optical components in the sub-picosecond regime," *Opt. Lett.* **40**, 2091–2094 (2015).
20. ISO Standard 21254-2, "Lasers and laser-related equipment—determination of laser-damage threshold of optical surfaces," *International Organization for Standardization* (2011).
21. M. Sozet et al., "Laser damage growth with picosecond pulses," *Opt. Lett.* **41**, 2342–2345 (2016).
22. M. Sozet et al., "Assessment of mono-shot measurement as a fast and accurate determination of the laser-induced damage threshold in the sub-picosecond regime," *Opt. Lett.* **41**, 804–807 (2016).
23. Spica Technologies, Inc., www.spicatech.com (15 August 2016).
24. "Small optics laser damage test procedure," NIF Technical Report MEL01-013-0D, Lawrence Livermore National Laboratory, Livermore, California (2005).
25. R. A. Negres et al., "Characterization of laser-induced damage by picosecond pulses on multi-layer dielectric coatings for petawatt-class lasers," *Proc. SPIE* **9632**, 963206 (2015).
26. L. Gallais, X. Cheng, and Z. Wang, "Influence of nodular defects on the laser damage resistance of optical coatings in the femtosecond regime," *Opt. Lett.* **39**, 1545–1548 (2014).

John Bellum received his BS (Georgia Institute of Technology, 1968) and PhD (University of Florida, 1976) degrees in physics. He has numerous scientific publications and extensive experience as a physicist and optical engineer. He provides technical leadership for the Large Optics Coating Facility at Sandia National Laboratories, specializing in high laser damage threshold optical coatings for large, meter-size optics for petawatt-class lasers. He is a senior member of both SPIE and OSA.

Trevor Winstone has worked at the Science and Technology Facility Council's (STFC) Rutherford Appleton Laboratory for the last 28 years operating the Vulcan Nd:Glass Laser system, undertaking major roles in optical quality assurance and operations management. He continues to push the boundaries of optical capability for high power lasers through with significant input to major projects: DiPOLE laser to HiLASE, Vulcan 10PW project and the HiPER project.

Laurent Lemaignère studied physics in the University of Bordeaux. After obtaining his PhD at the Centre de Recherches Paul Pascal, he had for 2 years a postdoctoral position at the CEA-CESTA. He has been working for CEA since 2000 on the laser damage topic in the framework of the Laser Megajoule and the PETAL laser. He is in charge of CEA laser damage metrology, and he supervises thesis dealing with the ns and fs laser damage issues.

Martin Sozet received his diploma from the engineering school Centrale Marseille, France, in 2013, and is currently preparing his PhD at the CEA CESTA, Bordeaux, and the Institut Fresnel, Marseille. His research interests are laser damage in the sub-picosecond regime and the design of optical components for petawatt applications.

Mark Kimmel has been involved in the area of optical science and engineering for more than 30 years at Sandia National Laboratories in Livermore, California, and Albuquerque, New Mexico, USA; and at the Georgia Institute of Technology in Atlanta, Georgia, USA. Primary research areas include optical damage studies, laser development, and the development of diagnostic techniques and instruments for the ultrafast phenomena and high energy density physics communities.

Patrick Rambo received his BA degree in applied physics from Rice University in 1993. He received his PhD in optical sciences from the University of New Mexico in 2000 for dissertation research on laser-triggered lightning. Since 2000, he has been at Sandia National Laboratories working mostly at the Z-Backlighter facility. He was part of the teams there which activated the kilojoule-class Z-Beamlet laser for radiography and which developed the Z-Petawatt system.

Ella Field is an engineer at Sandia National Laboratories in Albuquerque, New Mexico. She manages operations at the Optical Support Facility and develops optical coatings for the Z-Backlighter Laser. She received her bachelor's degrees in mechanical engineering and Asian languages and literature from the University of Minnesota in 2009 and received a master's degree in mechanical engineering from Massachusetts Institute of Technology in 2011.

Damon Kletecka is an optical coating technologist at Sandia National Laboratories in Albuquerque, New Mexico, USA. He has spent the past 12 out of 13 years at Sandia with the Large Optics Coating Facility, supporting the general operation and maintenance of the coating system.